


# Extending Our Knowledge about the $^{229}\text{Th}$ Nuclear Isomer

Benedict Seiferle \*, Daniel Moritz, Kevin Scharl, Shiqian Ding †, Florian Zacherl, Lilli Löbell and Peter G. Thirolf \* 

Faculty of Physics, Ludwig-Maximilians University München, Am Coulombwall 1, 85748 Garching, Germany; daniel.moritz@physik.uni-muenchen.de (D.M.); K.Scharl@physik.uni-muenchen.de (K.S.); dingshq@gmail.com (S.D.); Zacherl.Florian@physik.uni-muenchen.de (F.Z.); Lilli.Loebell@physik.uni-muenchen.de (L.L.)

\* Correspondence: benedict.seiferle@physik.uni-muenchen.de (B.S.); peter.thirolf@physik.uni-muenchen.de (P.G.T.)

† Current Address: Department of Physics, Tsinghua University, Beijing 100084, China.

**Abstract:** The first nuclear excited state in  $^{229}\text{Th}$  possesses the lowest excitation energy of all currently known nuclear levels. The energy difference between the ground- and first-excited (isomeric) state (denoted with  $^{229\text{m}}\text{Th}$ ) amounts only to  $\approx 8.2$  eV ( $\approx 151.2$  nm), which results in several interesting consequences: Since the excitation energy is in the same energy range as the binding energy of valence electrons, the lifetime of  $^{229\text{m}}\text{Th}$  is strongly influenced by the electronic structure of the Th atom or ion. Furthermore, it is possible to potentially excite the isomeric state in  $^{229}\text{Th}$  with laser radiation, which led to the proposal of a nuclear clock that could be used to search for new physics beyond the standard model. In this article, we will focus on recent technical developments in our group that will help to better understand the decay mechanisms of  $^{229\text{m}}\text{Th}$ , focusing primarily on measuring the radiative lifetime of the isomeric state.

**Keywords:** Th-229; nuclear clock; hyperfine structure spectroscopy; ion trap



**Citation:** Seiferle, B.; Moritz, D.; Scharl, K.; Ding, S.; Zacherl, F.; Löbell, L.; Thirolf, P.G. Extending Our Knowledge about the  $^{229}\text{Th}$  Nuclear Isomer. *Atoms* **2022**, *10*, 24. <https://doi.org/10.3390/atoms10010024>

Academic Editor: Camillo Mariani

Received: 31 December 2021

Accepted: 31 January 2022

Published: 14 February 2022

**Publisher's Note:** MDPI stays neutral with regard to jurisdictional claims in published maps and institutional affiliations.



**Copyright:** © 2022 by the authors. Licensee MDPI, Basel, Switzerland. This article is an open access article distributed under the terms and conditions of the Creative Commons Attribution (CC BY) license (<https://creativecommons.org/licenses/by/4.0/>).

## 1. Introduction

The nuclear first excited state in  $^{229}\text{Th}$  is in the focus of nuclear as well as atomic physics research. Due to its low excitation energy in the range of  $\approx 8.2$  eV (we took the mean value of the two most recent energy determinations [1,2]), the first nuclear excited state plays an exceptional role with the possibility to be excited by laser light. This led to the proposal to use the  $^{229}\text{Th}$  nucleus as a basis for a nuclear optical clock [3]. It has been predicted that a nuclear clock could potentially reach a relative frequency uncertainty in the range of  $10^{-19}$  [4]. Therefore, such a nuclear clock could complement current atomic clocks. It could especially be employed in the search for new physics beyond the standard model [5].

The reader is referred to the references [6–8] for a detailed overview of the topic.

The exceptionally low excitation energy plays an important role when one considers the possible decay channels of the isomer: The isomer potentially decays to its ground state via four decay channels:  $\gamma$  decay, internal conversion (IC), bound internal conversion (BIC) [9] and electronic bridge (EB) [10]. In the gamma decay channel, the isomer decays by emitting a photon that carries the excitation energy. The partial lifetime of this decay channel has been predicted to be in the range of  $10^3$  to  $10^4$  s [11,12].

The  $\gamma$ -decay channel competes with the internal conversion decay channel, whose lifetime has been measured in neutral atoms to be in the range of several microseconds [13], making it orders of magnitude faster than the  $\gamma$  decay. During the internal conversion decay, the energy of the isomeric state is transferred to the electronic shell and an electron is emitted into the vacuum. A prerequisite for the IC decay to occur is that the binding energy of one of the bound electrons (which is given by the ionization potential) is below

the isomeric excitation energy. For the specific case of  $^{229\text{m}}\text{Th}$ , the IC decay is already energetically forbidden for  $^{229\text{m}}\text{Th}^{1+}$  ions with an ionization potential of  $\approx 12$  eV.

Another possible decay channel is bound internal conversion, where the decay energy is also transferred to the electronic shell. Instead of an electron being emitted, as in the internal conversion decay, an electronic state is excited. A requirement for electronic bridge decay is the presence of a transition in the electronic shell that is in resonance with the isomeric ground-state transition. This strong requirement is relaxed in the electronic bridge channel, where the isomer decays by exciting a virtual state in the electronic shell, which subsequently decays to a real electronic state. The excess energy is then carried away in the form of photons.

In the following, we focus on prospects to measure the radiative decay channel in a new setup currently being arranged at LMU Munich.

## 2. Towards Radiative Lifetime Measurements

For the measurement of the radiative lifetime it is envisaged to monitor the number of  $^{229}\text{Th}$  ions in the isomeric state  $^{229\text{m}}\text{Th}$  over time. The measurement of the radiative lifetime requires the complete suppression of all the other competing decay channels, such as internal conversion and bound internal conversion. The suppression of internal conversion can be achieved by preventing  $^{229\text{m}}\text{Th}$  ions from neutralizing, since IC is energetically forbidden in Th ions. Therefore, the ions are confined in an ion trap. The trap is operated under cryogenic conditions to achieve the high vacuum quality that is needed to realize long storage times in the range of the expected radiative lifetime.

The appearance of BIC and EB can be excluded by measuring the lifetime in different electronic states. For a successful measurement of the lifetime, the storage time of the  $^{229(\text{m})}\text{Th}$  ions (the m in brackets indicates that we are dealing with a cloud of ions in the nuclear ground state and the nuclear isomeric state) in the ion trap needs to be at least in the range of the expected lifetime, i.e., several 1000 s. This requires optimum vacuum conditions that can only be achieved under cryogenic conditions at temperatures around 4 K.

The general concept of the setup is shown in Figure 1.  $^{229(\text{m})}\text{Th}^{3+}$  ions extracted from a buffer gas stopping cell are loaded axially (from the left side in Figure 1) into a cryogenic linear Paul trap.  $^{229(\text{m})}\text{Th}^{3+}$  ions are used due to their favorable electronic level scheme exhibiting a rather simple alkali-like structure of an inert Rn core and a single valence electron, providing a closed three-level Lambda system suitable for laser excitation and fluorescence detection. There, they are sympathetically cooled by  $^{88}\text{Sr}$  ions, which are provided by an ion source and are axially loaded into the same linear Paul trap from the opposite side (i.e., the right side in Figure 1).

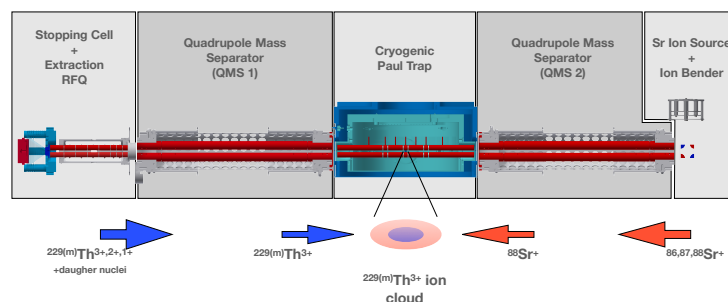


**Figure 1.** Visualization of the experimental setup and concept. A detailed explanation is provided in the text.  $^{229(\text{m})}\text{Th}$  ions are produced in the  $\alpha$ -decay of  $^{233}\text{U}$  and extracted by a buffer-gas stopping cell and an extraction radio frequency quadrupole (RFQ). A quadrupole mass separator (QMS) allows for the selection of a specific charge state, which enables the loading of  $^{229(\text{m})}\text{Th}^{3+}$  into a cryogenic Paul trap. Sr ions produced by an ion dispenser source are bent by  $90^\circ$  by an electrostatic ion bender and are then injected into a QMS that selects  $^{88}\text{Sr}^+$  from other naturally occurring Sr isotopes.  $^{88}\text{Sr}^+$  ions are loaded into the cryogenic Paul trap and can be laser cooled.

The Sr ion source is placed  $90^\circ$  off axis, and the ions are bent by  $90^\circ$  using an electrostatic bending quadrupole in order to prevent the cryogenic stages from being exposed to the heated ion source and thereby reducing the heat load to the cold stages. This geometry also allows for a direct line of sight along the central axis of the setup (e.g., to align lasers along the axis for Doppler cooling and spectroscopy).

### 2.1. Stopping Cell and Extraction RFQ

$^{229\text{(m)}}\text{Th}$  ions are produced in the  $\alpha$  decay of  $^{233}\text{U}$ , where the isomeric state is fed by a 2% decay branch. For this reason, a  $^{233}\text{U}$   $\alpha$  recoil source with an activity of 10 kBq is placed in a buffer-gas stopping cell. The source consists of a Si wafer disk with a diameter of 30 mm.  $^{233}\text{U}$  is deposited onto the disk by electroplating.  $^{229\text{(m)}}\text{Th}$  ions leaving the source material with a kinetic energy of  $\approx 84$  keV are stopped in 32 mbar catalytically purified helium. The ions are guided by an RF-DC funnel towards a de-Laval nozzle (nozzle diameter  $\varnothing = 0.4$  mm) that connects the high-pressure stopping cell to another vacuum chamber.

The RF-DC funnel consists of concentrically stacked ring electrodes, whose inner diameter is reduced linearly with the distance from the source, thus, creating a funnel-like shape. A DC gradient along the funnel electrodes guides the ions axially towards the de-Laval nozzle. Sinusoidal RF-fields that are varying in phase by  $180^\circ$  between neighboring funnel electrodes prevent the ions from hitting the electrodes. The electrical potentials together with the funnel-like geometry allow the transport of ions that are far from the central axis towards the nozzle exit.

In the vicinity of the de-Laval nozzle, a gas flow drags the ions through the nozzle and injects them into the subsequent chamber. The formed supersonic gas jet is generated by a pressure difference between the buffer-gas stopping cell (typically at 32 mbar) and the subsequent chamber, which is typically pumped to a pressure in the range of  $10^{-3}$ – $10^{-4}$  mbar.

This chamber houses an axially segmented radio-frequency quadrupole (RFQ). A voltage gradient along the axis drags the ions through the remaining buffer gas, while the applied RF voltage keeps the ions on the central axis. This enables the formation of a cooled ion beam.

### 2.2. Quadrupole Mass Separators

The setup contains two quadrupole mass separators (QMS 1 and 2). QMS 1 is used to generate an isotopically pure  $^{229\text{(m)}}\text{Th}^{3+}$  ion beam that can be injected into the Paul trap and is located between the extraction RFQ and the cryogenic Paul trap. The second QMS (QMS 2) is placed between the cryogenic Paul trap and the  $^{88}\text{Sr}$  ion source. QMS 2 serves two purposes: First, it is used to select  $^{88}\text{Sr}$  ions from the ion beam generated by the Sr ion source.

In addition to other naturally occurring Sr isotopes, the ion beam may also contain elements other than Sr (such as K, Rb or Cs) due to the production process of the source. Secondly, QMS 2 can be used to investigate a possible formation of molecules of the Th ions after being trapped in the Paul trap. The QMS modules follow the design of [14], which was also used in earlier experiments [1,13,15]. In order to achieve the required mass resolving power, the RF-voltage amplitudes are actively stabilized by an FPGA-based circuit. For further details, see [16].

### 2.3. Cryogenic Paul Trap

The central structure of the setup is a Paul trap that is designed to be operated at cryogenic conditions. The design of the Paul trap follows closely the design used in [17,18]. For further details, see [16].

#### 2.4. Sr Ion Source and Ion Bender

The Sr ion source is a commercially available heated dispenser ion source. The source is typically heated to a temperature above 1000 °C by applying a current of  $\approx 2.2$  A to a heating filament that is part of the source assembly.

The ions that are emitted from the source are extracted and focused by two ring electrodes. An electrostatic ion bender, consisting of four quarter cylinders that form a quadrupole potential, bends the ions by 90° towards QMS 2. Before entering QMS 2, the ions pass three more ring electrodes that help to efficiently inject them into QMS 2.

#### 2.5. Cooling Lasers and HFS Lasers

To resolve the hyperfine-structure (HFS) shifts that are used to distinguish between the nuclear ground and nuclear isomeric state the  $^{229\text{(m)}}\text{Th}^{3+}$  ions need to be cooled.

Direct laser cooling of  $^{229\text{(m)}}\text{Th}^{3+}$  has already been achieved [19]. In our setup,  $^{229\text{(m)}}\text{Th}^{3+}$  ions are sympathetically cooled by  $^{88}\text{Sr}$  ions, whose mass-to-charge ratio (88 u/e) is close to that of  $^{229\text{(m)}}\text{Th}^{3+}$  (76.3 u/e). The lack of hyperfine-structure shifts in  $^{88}\text{Sr}$  ions provides a simpler cooling scheme than for  $^{229\text{(m)}}\text{Th}^{3+}$ . Doppler cooling can be performed on the  $^2\text{S}_{1/2} \rightarrow ^2\text{P}_{1/2}$  transition at 422 nm [20]. The ions are re-pumped from the  $^2\text{D}_{3/2}$  to the  $^2\text{P}_{1/2}$  state with 1091 nm radiation (see the left part of Figure 2). The discrimination between the nuclear ground state and nuclear isomeric state is performed by measuring the HFS of  $^{229\text{(m)}}\text{Th}^{3+}$ .

The HFS will be probed on the  $^2\text{F}_{5/2} \rightarrow ^2\text{D}_{5/2}$  transition at 690 nm. An additional re-pumping laser at 984 nm is needed to pump from the  $^2\text{F}_{7/2}$  level back to  $^2\text{D}_{5/2}$ . The level scheme is shown in the right panel of Figure 2.  $^{229\text{(m)}}\text{Th}^{3+}$  exhibits a rich hyperfine structure; therefore, in order to avoid pumping into (hyperfine) dark-states, corresponding sidebands are generated with electro-optic modulators (EOMs). All central wavelengths are provided by external cavity diode lasers.

The 422 nm laser is locked to a close-by transition in Rb and shifted with an acousto-optical modulator (AOM) by approximately 440 MHz in order to drive the transition in  $^{88}\text{Sr}$  [21]. The remaining lasers will be stabilized by either using a scanning transfer cavity or a commercial wavelength meter.

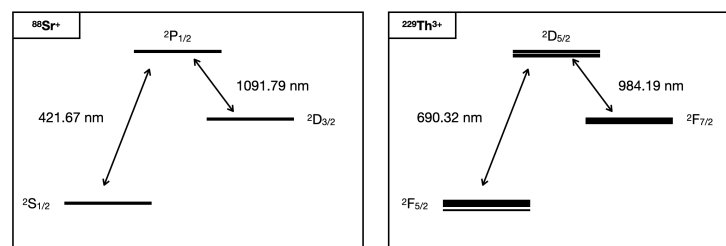


**Figure 2.** The relevant level schemes of singly charged  $^{88}\text{Sr}$  and triply charged  $^{229}\text{Th}$ . The presence of the hyperfine structure is indicated by the broadened width of the bars.

#### 2.6. Measurement Scheme

The measurement scheme involves two stages. Ions are loaded into the trap and cooled down in a first stage. The second stage involves the measurement of the lifetime. First,  $^{229\text{(m)}}\text{Th}^{3+}$  ions are loaded into the trap. The ions are extracted from a buffer gas stopping cell. We estimate the number of extracted ions by scaling the number of  $^{229\text{(m)}}\text{Th}^{3+}$  ions extracted from a similar buffer-gas stopping cell and a similar source geometry [15] with the source activity. In Ref. [15], the number of extracted  $^{229\text{(m)}}\text{Th}^{3+}$  ions was on the order of  $10^4$  ions per second with a source activity of 290 kBq. Therefore, we expect an extraction rate in the range of  $10^2$  ions per second.

This number, however, requires experimental verification, as the exact extraction rate is influenced by several factors, such as the buffer gas cleanliness. We expect a small number of  $^{229\text{(m)}}\text{Th}^{3+}$  ions in the range between 10 and 100 to be loaded into the trap. It is envisaged to form an ion crystal by sympathetic cooling and to identify the nuclear state

of the trapped ions by measuring their hyperfine structure. When there is at least one isomer confined in the trap, the lifetime measurement is started. This involves imaging the fluorescence radiation of individual ions onto an (EM)CCD camera.

This allows for identification of the decay of the isomer by tagging ions in the isomeric state on the camera image via their HFS fluorescence and registering their decay to the ground state; the lasers are set to exclusively drive HFS transitions that correspond to the isomeric state. When the isomeric state decays to the ground state, the respective thorium ion turns dark on the camera.

In order to double-check that the ion was not lost due to any other process (i.e., neutralization or molecule formation), the laser is set to drive nuclear ground-state HFS transitions immediately after the ion has turned dark. If the ion is still present in the trap, the time of the decay event can then be recorded and used for data analysis.

It is possible that the isomeric radiative lifetime is affected by the electronic state. For cross-checks, the duty-cycle of the 690 nm laser can be varied. This will leave the ions in the electronic ground-state for a variable amount of time. Additionally, by varying the duty cycle of the re-pumping laser (984 nm), it is possible to pump the ions into the  $^2F_{7/2}$  electronic state and investigate the isomeric lifetime for ions in this electronic excited state.

### 3. Conclusions

We presented a setup that is able to measure the radiative lifetime of  $^{229\text{m}}\text{Th}$  in the absence of the internal conversion decay channel. For this purpose, triply charged  $^{229(\text{m})}\text{Th}$  ions are confined in a cryogenic Paul trap.  $^{229(\text{m})}\text{Th}$  is cooled sympathetically by a laser-cooled cloud of  $^{88}\text{Sr}$  ions. The number of  $^{229\text{m}}\text{Th}$  ions is monitored over time by measuring the hyperfine-structure shifts specific for  $^{229\text{m}}\text{Th}$ .

**Author Contributions:** The original draft was prepared by B.S. with input from B.S., D.M., K.S., S.D., F.Z., L.L. and P.G.T.; supervision, P.G.T. All authors have read and agreed to the published version of the manuscript.

**Funding:** This work is part of the ‘ThoriumNuclearClock’ project that received funding from the European Research Council (ERC) under the European Union’s Horizon 2020 Research and Innovation Programme (Grant Agreement No. 856415) and by the European Union’s Horizon 2020 Research and Innovation Programme under grant agreement No 664732 “nuClock”.

**Institutional Review Board Statement:** Not applicable.

**Informed Consent Statement:** Not applicable.

**Data Availability Statement:** Not applicable.

**Acknowledgments:** We thank J. R. Crespo López-Urrutia, E. Peik, M. Okhapkin, J. Thielking, J. Weitenberg and L. v.d. Wense for fruitful discussions and their support.

**Conflicts of Interest:** The authors declare no conflict of interest.

### References

1. Seiferle, B.; von der Wense, L.; Bilous, P.V.; Amersdorffer, I.; Lemell, C.; Libisch, F.; Stellmer, S.; Schumm, T.; Düllmann, C.E.; Pálffy, A.; et al. Energy of the  $^{229}\text{Th}$  nuclear clock transition. *Nature* **2019**, *573*, 243–246. [[CrossRef](#)] [[PubMed](#)]
2. Sikorsky, T.; Geist, J.; Hengstler, D.; Kempf, S.; Gastaldo, L.; Enss, C.; Mokry, C.; Runke, J.; Düllmann, C.E.; Wobrauschek, P.; et al. Measurement of the  $^{229}\text{Th}$  Isomer Energy with a Magnetic Microcalorimeter. *Phys. Rev. Lett.* **2020**, *125*, 142503. [[CrossRef](#)] [[PubMed](#)]
3. Peik, E.; Tamm, C. Nuclear laser spectroscopy of the 3.5 eV transition in Th-229. *Europhys. Lett.* **2003**, *61*, 181. [[CrossRef](#)]
4. Campbell, C.J.; Radnaev, A.G.; Kuzmich, A.; Dzuba, V.A.; Flambaum, V.V.; Derevianko, A. Single-Ion Nuclear Clock for Metrology at the 19th Decimal Place. *Phys. Rev. Lett.* **2012**, *108*, 120802. [[CrossRef](#)] [[PubMed](#)]
5. Peik, E.; Schumm, T.; Safronova, M.S.; Pálffy, A.; Weitenberg, J.; Thierolf, P.G. Nuclear clocks for testing fundamental physics. *Quantum Sci. Technol.* **2021**, *6*, 034002. [[CrossRef](#)]
6. Thierolf, P.G.; Seiferle, B.; von der Wense, L. The 229-thorium isomer: Doorway to the road from the atomic clock to the nuclear clock. *J. Phys. B At. Mol. Opt. Phys.* **2019**, *52*, 203001. [[CrossRef](#)]

7. Thirolf, P.G.; Seiferle, B.; von der Wense, L. Fundamental Constants: Improving Our Knowledge on the  $^{229m}\text{Th}$  Isomer: Toward a Test Bench for Time Variations of Fundamental Constants (Ann. Phys. 5/2019). *Ann. Der Phys.* **2019**, *531*, 1800381. [[CrossRef](#)]
8. Beeks, K.; Sikorsky, T.; Schumm, T.; Thielking, J.; Okhapkin, M.V.; Peiket, E. The thorium-229 low-energy isomer and the nuclear clock. *Nat. Rev. Phys.* **2021**, *3*, 238–248. [[CrossRef](#)]
9. Karpeshin, F.F.; Trzhaskovskaya, M.B. Bound internal conversion versus nuclear excitation by electron transition: Revision of the theory of optical pumping of the  $^{229m}\text{Th}$  isomer. *Phys. Rev. C* **2017**, *95*, 034310. [[CrossRef](#)]
10. Strizhov, V.F.; Tkalya, E.V. Decay channel of low-lying isomer state of the Th-229 nucleus. Possibilities of experimental investigation. *Sov. Phys. JETP* **1991**, *72*, 387.
11. Tkalya, E.V.; Schneider, C.; Jeet, J.; Hudson, E.R. Radiative lifetime and energy of the low-energy isomeric level in  $^{229}\text{Th}$ . *Phys. Rev. C* **2015**, *92*, 054324. [[CrossRef](#)]
12. Minkov, N.; Pálffy, A. Reduced Transition Probabilities for the Gamma Decay of the 7.8 eV Isomer in  $^{229}\text{Th}$ . *Phys. Rev. Lett.* **2017**, *118*, 212501. [[CrossRef](#)] [[PubMed](#)]
13. Seiferle, B.; von der Wense, L.; Thirolf, P.G. Lifetime Measurement of the  $^{229}\text{Th}$  Nuclear Isomer. *Phys. Rev. Lett.* **2017**, *118*, 042501. [[CrossRef](#)] [[PubMed](#)]
14. Haettner, E.; Plaß, W.R.; Czok, U.; Dickel, T.; Geissel, H.; Kinsel, W.; Petrick, M.; Schäfer, T.; Scheidenberger, C. A versatile triple radiofrequency quadrupole system for cooling, mass separation and bunching of exotic nuclei. *Nucl. Instrum. Methods A* **2018**, *880*, 138–151. [[CrossRef](#)]
15. von der Wense, L.; Seiferle, B.; Laatiaoui, M.; Neumayr, J.B.; Maier, H.-J.; Wirth, H.-F.; Mokry, C.; Mokry, J.; Eberhardt, K.; Düllmann, C.E.; et al. Direct detection of the  $^{229}\text{Th}$  nuclear clock transition. *Nature* **2016**, *533*, 47–51. [[CrossRef](#)] [[PubMed](#)]
16. Moritz, D.; Scharl, K.; Ding, S.; Seiferle, B.; von der Wense, L.; Zacherl, F.; Löbell, L.; Thirolf, P.G. A cryogenic Paul trap setup for the determination of the ionic radiative lifetime of  $^{229}\text{Th}^{3+}$ . 2022, *in preparation*.
17. Schwarz, M.; Versolato, O.O.; Windberger, A.; Brunner, F.R.; Ballance, T.; Eberle, S.N.; Ullrich, J.; Schmidt, P.O.; Hansen, A.K.; Gingell, A.D.; et al. Cryogenic linear Paul trap for cold highly charged ion experiments. *Rev. Sci. Instrum.* **2012**, *83*, 083115. [[CrossRef](#)] [[PubMed](#)]
18. Leopold, T.; King, S.A.; Micke, P.; Bautista-Salvador, A.; Heip, J.C.; Ospelkaus, C.; Crespo López-Urrutia, J.R.; Schmidt, P.O. A cryogenic radio-frequency ion trap for quantum logic spectroscopy of highly charged ions. *Rev. Sci. Instrum.* **2019**, *90*, 073201. [[CrossRef](#)] [[PubMed](#)]
19. Campbell, C.J.; Radnaev, A.G.; Kuzmich, A. Wigner Crystals of  $^{229}\text{Th}$  for Optical Excitation of the Nuclear Isomer. *Phys. Rev. Lett.* **2011**, *106*, 223001. [[CrossRef](#)] [[PubMed](#)]
20. Removille, S.; Dubessy, R.; Dubost, B.; Glorieux, Q.; Coudreau, T.; Guibal, S.; Likforman, J.-P.; Guidoni, L. Trapping and cooling of  $\text{Sr}^+$  ions: Strings and large clouds. *J. Phys. B At. Mol. Opt. Phys.* **2009**, *42*, 154014. [[CrossRef](#)]
21. Madej, A.A.; Marmet, L.; Bernard, J.E. Rb atomic absorption line reference for single  $\text{Sr}^+$  laser cooling systems. *Appl. Phys. B* **1998**, *67*, 229–234. [[CrossRef](#)]